COMPUTATIONAL DESIGNING OF DEFERIPRONE BASED NOVEL DRUGS AS EFFICIENT *ANTI-PARKINSON* AGENTS

A.U. HASSAN†, N. K. NKUNGLI§ and C. GULERYUZ‡

† *University of Gujrat, Faculty of Science, Department of Chemistry, 50700 Gujrat, Pakistan*
hassanabrar2016@gmail.com
§ *The University of Bamenda, Department of Chemistry, Faculty of Science, P.O. Box 39, Bambili-Bamenda, Cameroon*
‡ *Department of Opticianry, Altınbaş University, 34144 İstanbul, Turkey*

***Abstract*— Comprehensive and detailed density functional theory (DFT) computations are done herein at the M05-2X/6-31G(d) level of theory to scrutinize the interactions of Fe^{3+} ions with computationally designed deferiprone (DFP)-based novel complexing drugs. The thermodynamic properties of metal-deferiprone complexes were determined in water as solvent. The theoretical binding energy trend indicated that $[Fe(DrugC)_3]$ has the highest interaction affinity. Natural bond orbital (NBO) analysis was used to estimate and assess atomic natural charges, the charge transfer between metal ions with ligands (oxygen atoms), and the interaction energy (E(2)) levels. The determined value of E(2) (donor-acceptor interaction energy) for the $[Fe(DrugC)_3]$ complex was greater than those of the other complexes. The understudy novel chelators were made to interact with graphidyne based nanosheet to understand their adsorption behavior. Interestingly, π---CH interaction of the complexes with the nanosheet were found around (2.41-3.12A), which endorsed their good behavior. The quantum theory of atoms in molecules (QTAIM) analysis was used to establish the type of efficient interactions and bonding characteristics in water. Based on the QTAIM results, $[Fe(DrugC)_3]$ was found to have the strongest M-O bond. The M-O bonds in the compounds were non-covalent, whereas they were electrostatic or partially covalent in all other complexes.**

***Keywords*— Binding energy, DFT, NBO, Nanosheet**

I. INTRODUCTION

Parkinson's disease (PD) is a neurodegenerative ailment that disrupts basic everyday skills and finally leads to a full impairment of cognition due to iron accumulation (ul Hassan *et al.*, 2016). With a rapidly rising prevalence, PD is currently estimated to be responsible for most serious public health and socioeconomic crises confronting the aged (Sharabi *et al.*, 2021). Metal ions are necessary for a wide range of biological processes in living systems, including metabolic regulation (Arjmand *et al.*, 2019). Despite their usefulness in many sectors, when their concentrations exceeds natural levels, they might become hazardous (Hassan *et al.*, 2017). Indeed, excessive amounts of metal ions can build up in critical organs including the brain, liver, and kidneys, resulting in the production of reactive oxygen species (ROS) (Vats *et al.*, 2021). Iron is the most prevalent transition metal in the Earth's crust, and it is required for a variety of biological activities (Abou-Elela *et al.*, 2021). Despite these benefits, excessive amounts of iron in the body can lead to iron overload syndrome, which can cause tissue damages and mortality (Ndagi *et al.*, 2017).

Chelating compounds containing oxygen substituents have a wide range of pharmacological uses in medicine, including iron overload (Sorouraddin *et al.*, 2020). A chelating agent must have a good specificity and affinity for the harmful metal ions it is meant to remove (Hassan *et al.*, 2018). Attributed to the prevalence of multiple donor atoms, polydentate chelating drugs create a more stable complex than monodentate chelating agents. The changes in the frequency and strength of chelate rings can help to enhance stability by reducing steric strain. Many chelate rings for protonated and tridentate chelating compounds include five or six members. The investigation of metal-ligand complexes with the form of bonding offers broad knowledge of metal ion binding and responsiveness. The ferriprox is one of the most significant families of 3-hydroxypyridin-4-ones (HPOs), which is octahedral to metal ions in a 3:1 molar ratio (Chaudhary *et al.*, 2021). Identifying the bonding characteristics of metal ions with ligands and biological molecules is crucial in the biological field, where complexes have several uses.

Metal ion absorption by biological molecules is by far the most critical event in living cells (Hassan *et al.*, 2017), and computational modeling is a vital tool for investigating chemical and biological phenomena. The binding of Fe(II) to a novel series of DFP-based, computationally designed drugs has been studied using theoretical approaches in the present research to develop the competent candidates for iron chelation and removal during PD therapy.

II. COMPUTATIONAL METHODS

The M05-2X functional in conjunction with the 6-31G(d) basis set in water as solvent was used to fully optimize the geometries of the complexes, and the isolated ligand (DFP) (Ekennia *et al.*, 2017). As per Hohenstein research, the M05-2X functional is superior to the other exchange-correlation functionals in terms of non-covalent relationships(Seritan *et al.*, 2021). The Gaussian 09 pack-

age was used for all quantum chemical computations. Vibrational frequency analysis was performed at the above-mentioned level of theory to estimate the thermodynamics functions and validate the optimized geometries as energy field minima. The thermodynamics parameters were determined at 298.15 K and pH = 7.4. Because of the relevance of these substances in biological processes, all computations were carried out in aqueous solvent, which is represented by means of the conductor-like polarizable continuum model (CPCM). Natural Bond Orbital (NBO) analysis was performed on the optimized structures to identify the electronic properties of the complexes and to determine their key donor-acceptor interactions.

DFT studies were performed on the translating coordinates from each complex enabling molecular relaxing simulations (with and without metal ions). For relaxing, the kinetic energy cut-off of each complex was employed, and the biggest visible energy cut-off has been used. The optimized morphologies of the relaxed complexes had been then used in total energy computations to calculate binding affinity, which was given by the equation:

$$E_{bindig} = (E_{metal + substrate} - E_{metal} - E_{substrate}) \quad (1)$$

The following equation was used to analyze charge transfer from metal interaction to ligand surfaces:

$$\rho_{bindig} = (\rho_{metal + substrate} - \rho_{metal} - \rho_{substrate}) \quad (2)$$

In multi-functional ligands, drug likeness is a significant parameter for determining appropriate pharmacokinetic characteristics. Lipinski's rule of five is commonly used to evaluate these properties which states that is ideal for drug-like compounds if it meets the criteria. Drug-likeness of novel compounds was studied by using molinspiration online facility (Guechtouli *et al.*, 2019).

III. GEOMETRICAL PARAMETERS

The Fe–N bond lengths which were determined on the optimal configuration during our study ranged between 2.013, 2.12, and 2.14 Å. Previous studies on similar Cu–Ab compounds employing Cu attached to His6, His13, and His14 yielded Cu–N bond length of 2.03, 2.03, and 2.07, respectively (Tosato and Di Marco, 2019). This demonstrates that the Fe–N bond lengths throughout this study are equivalent to those in prior research. When contrasted to some other materials, the binding energy distribution of such metal complexes revealed that the investigated binding site had the maximum affinity for aluminium. The computed binding energy energies are in the following order: $[Fe(DrugC)_3]$ > $[Fe(DrugA)_3]$ > $[Fe(DrugB)_3]$. To be considered for future PD treatment applications, a metal–chelator complex must have a binding energy higher than the comparable metal–AB complex (Liu and Luo, 2021).

IV. STRUCTRE AND BONDING

The optimized geometries of the metal-deferiprone complexes are shown in Fig. 1. Inspection of the bond lengths in the free ligand and the corresponding complexes reveals that the presence of the various ions leads to increments in bond lengths (Hassan *et al.*, 2022). Furthermore, the average Fe-O bond lengths in the complexes was 1.97

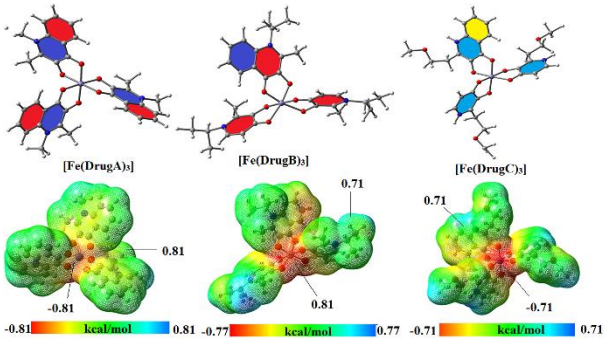

Figure 1: Optimized geometries and electrostatically mapped surfaces of novel drug complexes.

Table 1. Binding affinities of computationally designed compounds

Compounds	E_b(Ha)	E_b (kcal mol^{-1})
Drug-A	0.021	13.1777
Drug-B	0.032	20.0803
Drug-C	0.013	8.157
$[Fe(DrugA)_3]$	0.035	21.96
$[Fe(DrugA)_3]$	0.038	23.8454
$[Fe(DrugA)_3]$	0.016	10.420

demonstrating that the interaction between Fe^{+2} and DrugC was greater than that of other metal complexes. The energies of highest occupied molecular orbital (HOMO) and lowest unoccupied molecular orbital (LUMO) were estimated in a bid to assess the stability and reactivity of the compounds investigated. The HOMO–LUMO energy gap (E_{gap}) is the disparity in energy between the HOMO and LUMO. A high charge location suggests that the molecule is more chemically stable or has less chemical reactivity.

The $[Fe(DrugB)_3]$ value of 0.252 a.u., indicating that it has lesser biological activity and higher chemical inertness than other complexes. A decrease in E_{gap} is linked to an increase in the M–O bond length (Zampar *et al.*, 2020). Furthermore, we discovered that the length of the M–O bond in metal ions was indeed longer than that of trivalent cations (Yufanyi *et al.*, 2020). The binding (*E*) characteristics of complexes were correlated to their stabilization. The durability of complexes in water increased as the absolute binding energy levels improved (Muhsan *et al.*, 2019). These findings suggest that the charge transfer among drugs and their metal complexes should be increased.

Interpretivist density functional theory (DFT) based global reactivity markers have been employed to determine the relationship among structural system, coherence, and global surface sciences (Aydın *et al.*, 2020). The complexation binding enthalpy (H_{bind}) demonstrates that the association amid deferiprone based drugs and understudy metal ions is altered by thermal adjustments in water.

Quantitative structure-activity (QSAR), structure property (QSPR), and structure toxicity (QSTR) connections have all been created using these designations. The most important chemical property, electronegativity, characterizes a species with its ability to obtain electrons for itself (Hassan *et al.*, 2022). The values arranged in the

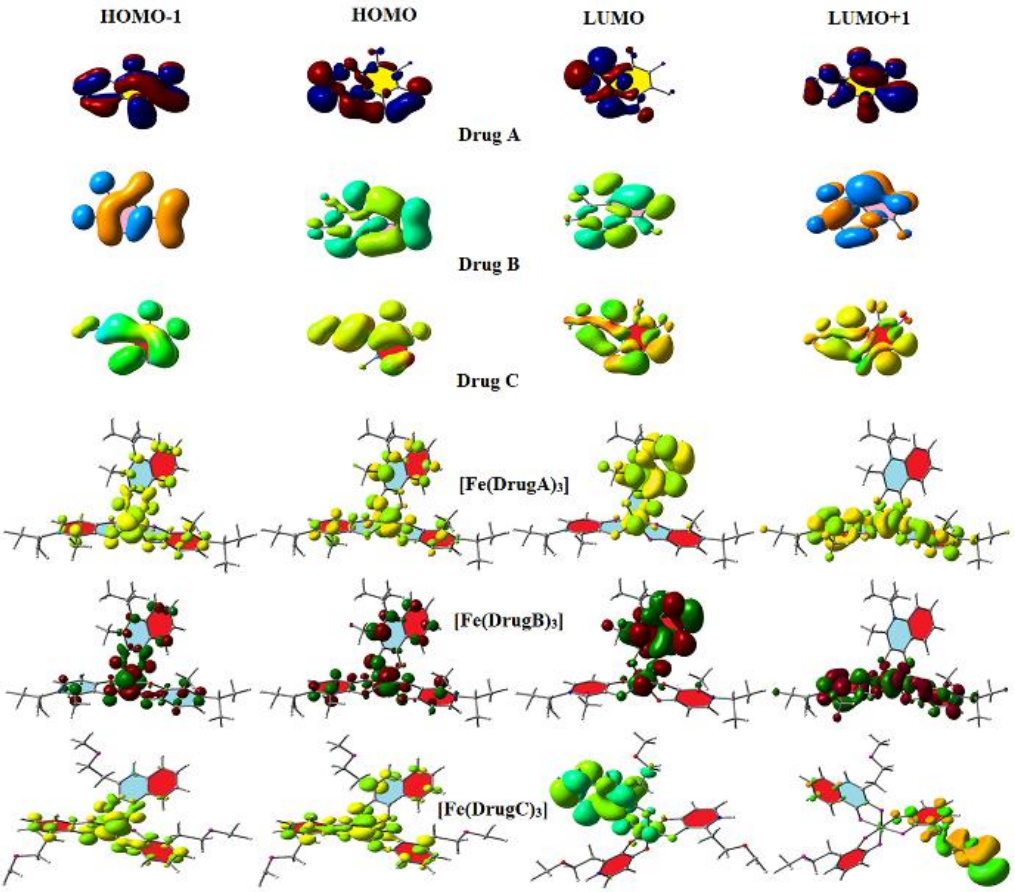

Figure 2: Charge density analysis of computationally designed drugs and metal complexes

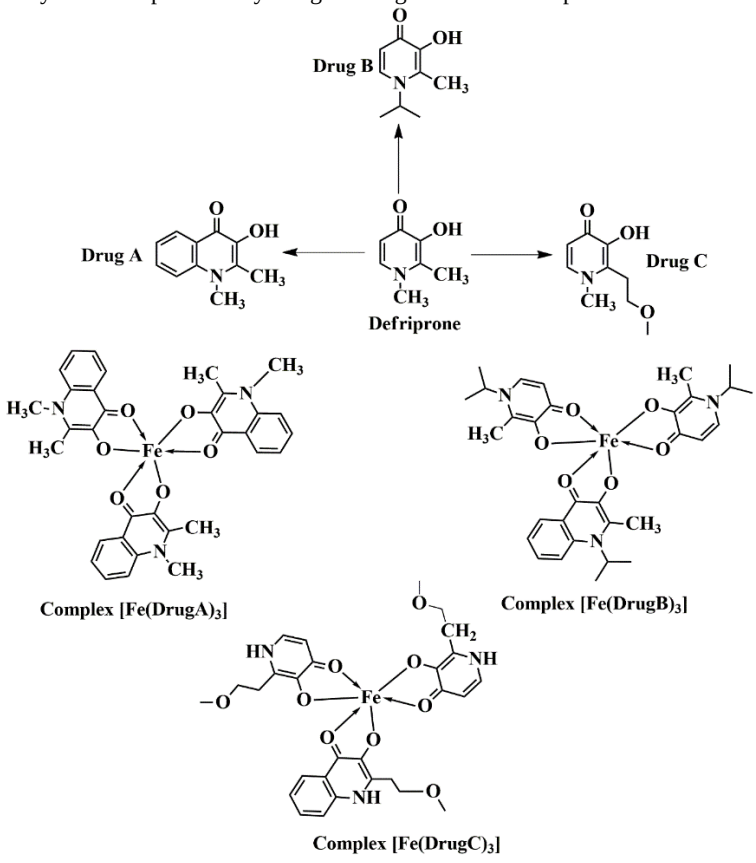

Figure 3. Theoretical designing of Deferiprone derived drugs as metal chelators.

Table 2. Quantum chemistry of computationally studied compounds

No	DA	DB	DC	FeA	FeB	FeC
E_H	*-1.86*	*-3.22*	-3.22	*-5.45*	*-4.90*	-4.74
E_L	*-0.75*	*-0.97*	*-0.88*	*-5.09*	*-4.24*	-4.24
E_{H-L}	*1.11*	*2.25*	*2.34*	*0.36*	*0.66*	*0.50*
(*IP*)	1.86	3.22	3.22	5.45	4.90	4.74
(*EA*)	0.75	0.97	0.88	5.09	4.24	4.24
(χ)	1.31	2.10	2.05	5.27	4.57	4.49
(μ)	-1.31	-2.10	-2.05	-5.27	-4.57	-4.49
(η)	0.56	1.13	1.17	0.18	0.33	0.25
(*S*)	0.90	0.44	0.43	2.82	1.52	2.00
(ω)	1.53	1.95	1.79	78.16	31.64	40.32

following order: **DA > DB = DC > Fe(C)$_3$ > Fe(B)$_3$ > Fe(A)$_3$**. When comparing to the complexes, the drugs showed greater electronegativity, implying that they were more reactive. A product with its aromaticity is proportional to its (η).

The (η) sign represents electrons' proclivity to leave the electronic atmosphere. It also shows the level of electronic cloud distortion dispute.

All the compounds were arranged in the following order: **DA > DC > DB > Fe(B)$_3$ = Fe(C)$_3$ > Fe(A)$_3$.** Whenever the unit becomes saturated with electrons following the external circumstances, the (ω) reflects the reliability potential. The compounds were listed in the following order: **DC > DB > DA > Fe(B)$_3$ > Fe(C)$_3$ > Fe(A)$_3$.** The calculated findings for global hardness inside the investigated compounds were stronger than those of metal complexes, suggesting that the examined drugs were less aggressive than respective metal complex counterparts (Table 2).

The hardness scores and the decreasing trend of FMO energy band gap were found to be same. The relative order for softness and hardness was recorded as respectively: Fe(C)$_3$ > Fe(A)$_3$ > Fe(B)$_3$ > DB = DA > DC and DC > DB > DA > Fe(B)$_3$ > Fe(A)$_3$ > Fe(C)$_3$. The DFT had already played a role in laying the theoretical basis for standard biochemical terminology consistency. Many quantum chemical reactivity motifs, including site selectivity, were also suggested, and utilized to assess chemical characteristics.

V. NATURAL BOND ORBITAL ANALYSIS

The origin of affiliations between metal cations and electron-donating O atoms of deferiprone may be electrostatic, as shown in a QTAIM investigation (Bine *et al.*, 2018). The metal ion polarity of the M-O bond is confirmed by atomic energies on oxygen atoms of deferiprone as well as metal ions. When the M-O bond lengths of free ligands and complexes were being compared, a similar pattern emerges. The atomic competing values with both the oxygen atoms of the ligand and complex were used to assess the cost of charge transfers (qi). The highest charge transfer, pertaining to the computed E_{bind} values, was in [Al(DFP)$_3$] (0.07e) (qi). When the volume of the metal cation reduces, charge transfer rises. The second-order perturbation energies, E(2), of the direct interaction were calculated all throughout complex growth. The most critical energies of such complexes are connected to correlations between the oxygen lone pair electrons (LPO) and the metal ion non - bonding orbital (LP*M). The stronger the donor-acceptor contact, the higher the interaction energy observations, denoting a bigger charge transfer as from ligand with donor oxygens to the acceptor metal ions. The complex's computed E(2) value (224.77 kcal mol1) is greater than other complexes. This supports the greater DFP-Fe^{3+} interactions (Wiesbrock and Schmidbaur, 2003).

VI. ADSORPTION ANALYSIS

Figure 1 depicts the optimal arrangement of a BN-yne nanostructure, indicating that two kinds of B or N atoms may be distinguished. The B atom does have a higher positive charge than the B atom since the B atom is linked to triple electronegative Nitrogen atom, which draw more electron density, whereas the B atom is attached to two Nitrogen atom. The electron density estimates of M-O bonds are bigger than those of Fe-O, indicating that Fe-O bonds have the most engagement with deferiprone when compared to other metal ions. The bond critical sites of the M-O display positive values suggesting an electron density depletion, which is a feature of the non-covalent interactions. Consequently, at the vicinity of M-O bonds in [Fe(D)$_3$] compounds, purely theoretical ratios of -G(r)/V(r) > 1 and H(r) > 0 demonstrate those are non-covalent bonds.

VII. DRUG LIKENESS

Modern medical fast uptake and distribution is essential for its metabolic pathways and action to operate effectively (Guechtouli *et al.*, 2019). Additionally, toxic effects, which often takes a back seat to ADME activity, is a critical consideration. This is owing to that most of drugs that lose in clinical trials due to high toxicity are very restrictive and damaging in pharmacological engineering (Hassan and Mohyuddin, 2017). Computer - aided drug prediction combined with ADMET properties modelling during the drug design process should provide a wealth of opportunities for accelerating lead compound testing with predicted bioactivity (Fig. 3). The detailed analysis of a structure with its physio-chemical or structural features to identify the compound's potential as an oral drug-like candidate is known as drug likeness. To guarantee that the antagonists were of greater quality for subsequent leading refining, five filters have been used. All the well drug-like criteria were found to be followed by the molecule (Table 3). The drug's access of rotatable bonds suggested that it could be a candidate for responsive inhibition. Inhibitors are considered to offset point mutations that diminish inhibitor contact affinity by acquiring several other roles at various regions of the targeted proteins

The Octanol-water partition coefficient (miLogP) was lower than five (2.83-3.68), indicating increased solubility and robust penetration across the cell surface. As demonstrated by the negative (-0.43 to -0.93 cm/s), their effect of specific compounds was found to be infiltrated the skin. The total surface area of the polar areas (TPSA)

.
Table 3: NBO analysis of newly designed drugs

Factor	Deferiprone	A	B	C	Drug A	Drug A
miLog$_P$	-0.60	0.87	0.14	-0.42	1.78	0.74
TPSA	42.23	42.23	42.23	51.47	76.01	76.01
n_{atoms}	10.00	14.00	12.00	13.00	43.00	41.00
MW	139.15	189.21	167.21	183.21	620.46	604.50
n_{ON}	3.00	3.00	3.00	4.00	9.00	9.00
n_{OHNH}	1.00	1.00	1.00	1.00	0.00	0.00
$n_{violations}$	0.00	0.00	0.00	0.00	0.00	0.00
n_{rotb}	0.00	0.00	1.00	3.00	0.00	3.00
Volume	129.53	173.53	162.92	172.12	521.57	533.75

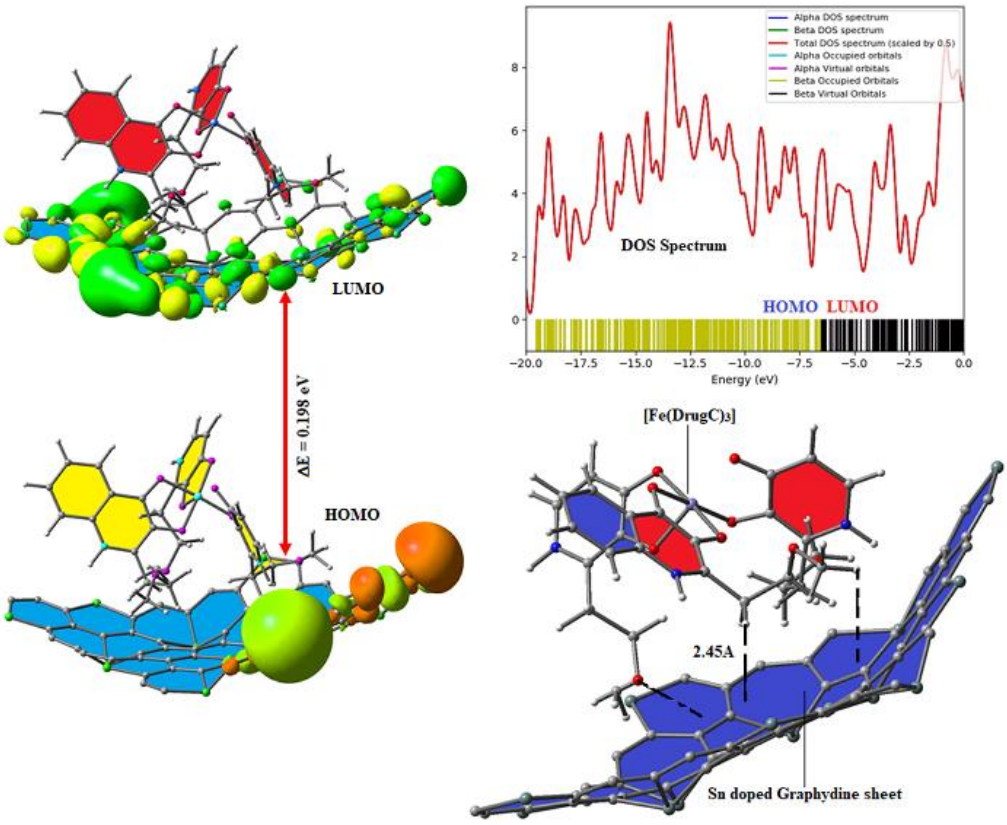

Figure 4: Adsorption, DOOs and charge density analysis of [Fe(DrugC)3] with graphydine 1D nanosheet

properties indicate that they can dissolve well to bind for a specific purpose when used as medications. It varied from 42.3 to 136.23 for presently designed drugs. Drugs were shown to have a lower value, whereas complexes had the greatest.

VIII. CONCLUSIONS

The selective complexation of deferiprone to different metal ions in water was demonstrated in this study using DFT calculations. The [(DFP)$_3$] complex is the most stable configuration among metal complexes, according to calculations. In comparison to certain other metal complexes, NBO research implies that the most stable structure of these organizations is the lone pair electrons of such deferiprone oxygens with various metal ions complexes. So according NBO investigation, such linkages were made by the lone pair of electrons by oxygen atoms. Furthermore, the links are non-covalent and involve charge transfer from the oxygen atoms of the ligand to the metal ion center. The positive value of 2 (r) at the affiliated metals indicated that the couplings between both the ligand's oxygen and nitrogen atoms, and the metal ion, were non-covalent. Furthermore, the ratios of -G(r)/V(r) at BCPs of the MO bond in [Fe(DC)$_3$] complex show that they have been noncovalent bonds, whereas they are electrostatic bonds and partially cohesive in other complexes.

REFERENCES

Abou-Elela, S.I., Fawzy, M.E. and El-Shafai, S.A. (2021) Treatment of hazardous wastewater generated from metal finishing and electro-coating industry via self-coagulation: Case study. *Water Environment Research.* **93**, 1476-1486.

Arjmand, F., Afsan, Z., Sharma, S., Parveen, S., Yousuf, I., Sartaj, S., Siddique, H.R. ans Tabassum, S. (2019) Recent advances in metallodrug-like molecules targeting non-coding RNAs in cancer

chemotherapy. *Coordination Chemistry Reviews*. **387**, 47–59.

Aydın, G., Koçak, O., Güleryüz, C. and Yavuz, I. (2020) Structural order and charge transfer in highly strained carbon nanobelts. *New J. Chem.* **44**, 15769–15775.

Bine, F.K., Nkungly, N.K., Numbonui, T.S. and Ghogumu, J.N. (2018) Structural Properties and Reactive Site Selectivity of Some Transition Metal Complexes of 2, 2′(1E, 1′ E)-(ethane-1, 2-diylbis (azan-1-yl-1-ylidene)) bis (phenylmethan-1-yl-1-ylidene) dibenzoic Acid: DFT, Conceptual DFT, QTAIM, and MEP Studies. *Bioinorganic chemistry and applications*. **2018,** 4510648.

Ekennia, A.C., Osowole, A.A., Olasunkanmi, L.O., Onwudiwe, D.C. and Ebenso, E.E. (2017) Coordination behaviours of new (bidentate N,O-chelating) Schiff bases towards copper(II) and nickel(II) metal ions: synthesis, characterization, antimicrobial, antioxidant, and DFT studies. *Research on Chemical Intermediates*. **43**, 3787–3811.

Guechtouli, N., Zaater, S., Kichou, N., Bouaziz-Terrachet, S. and Meghezzi, H. (2019) Theoretical investigation of dicarboxamide mono copper (II) and novel transition metal complexes: Structural, chemical reactivity, vibrational and in-silico biological analysis. *Journal of Molecular Structure*. **1188**, 23–30.

Hassan, A.U., Ali, S., Muhsen, S. and Rizwan, M. (2017) Heavy metal content of refined and bakery salts consumed in Pakistan. *Pakistan Journal of Scientific and Industrial Research Series A: Physical Sciences*. **60**, 172-174.

Hassan, A.U., Mohyuddin, A., Nadeem, S., Güleryüz, C., Hassan, S.U., Javed, M. and Muhsan, M.S. (2022) Structural and Electronic (Absorption and Fluorescence) Properties of a Stable Triplet Diphenylcarbene: A DFT Study. *Journal of Fluorescence*. **32**, 1629–1638.

Hassan, A.U. and Mohyuddin, A. (2017) Conformational and Drug-Receptor Binding Optimization Studies of Ergocalciferol (Vitamin D2) as a Potential Metabolic Antagonist. *Vitamins & Minerals*. **06**, 3–7.

Hassan, A.U., Mohyuddin, A. and Ali, S. (2018) Preparation of rechargeable battery from poultry waste. *Pakistan Journal of Scientific and Industrial Research Series A: Physical Sciences*. **61**, 80-83.

Liu, C. and Luo, X. (2021) Potential molecular and graphene oxide chelators to dissolve amyloid-$β$ plaques in Alzheimer's disease: a density functional theory study. *Journal of Materials Chemistry B*. **9**, 2736–2746.

Muhsan, M.S., Nadeem, S., Hassan, A.U., Udd Din, A.M., Shahid, S. and Ali, S. (2019) Synthesis of carbon nanoparticles by using seed oils. *Pakistan Journal of Scientific and Industrial Research Series A: Physical Sciences*. **62A**, 1–7.

Ndagi, U., Mhlongo, N. and Soliman, M.E. (2017) Metal complexes in cancer therapy--an update from drug design perspective. *Drug design, development and therapy*. **11**, 599-616.

Seritan, S., Bannwarth, C., Fales, B.S., Hohenstein, E.G., Isborn, C.M., Kokkila-Schumacher, S.I.L., Li, X., Liu, F., Luehr, N., Snyder Jr., J.W., Song, C., Titov, A.V., Ufimtsev, I.S., Wang, L.-P. and Martínez, T.J. (2021) TeraChem: A graphical processing unit-accelerated electronic structure package for large-scale ab initio molecular dynamics. *Wiley Interdisciplinary Reviews: Computational Molecular Science*. **11**, e1494.

Sharabi, Y., Vatine, G.D. and Ashkenazi, A. (2021) Parkinson's disease outside the brain: targeting the autonomic nervous system. *The Lancet Neurology*, **20**, 868–876.

Sorouraddin, S.M., Farajzadeh, M.A. and Dastoori, H. (2020) Development of a dispersive liquid-liquid microextraction method based on a ternary deep eutectic solvent as chelating agent and extraction solvent for preconcentration of heavy metals from milk samples. *Talanta*. **208**, 120485.

Tosato, M. and Di Marco, V. (2019) Metal chelation therapy and Parkinson's disease: A critical review on the thermodynamics of complex formation between relevant metal ions and promising or established drugs. *Biomolecules*. **9**, 269.

ul Hassan, A., Ali, S., Udd Din, A.M. and Muhsen, S. (2016) Chemical Characterisation of Unrefined Rock Salt Deposits of Pakistan. *Pakistan Journal of Scientific \& Industrial Research Series A: Physical Sciences*. **59**, 126–129.

Vats, S., Sudhakaran, S., Bhardwaj, A., Mandlik, R., Sharma, Y., Kumar, S., Tripathi, D.K., Sonah, H., Sharma, T.R. and Deshmukh, R. (2021) Targeting aquaporins to alleviate hazardous metal (loid) s imposed stress in plants. *Journal of Hazardous Materials*. **408**, 124910.

Wiesbrock, F. and Schmidbaur, H. (2003) Complexity of coordinative bonding in thallium(I) anthranilates and salicylates. *Journal of the American Chemical Society*. **125**, 3622–3630.

Yufanyi, D.M., Abbo, H.S., Titinchi, S.J.J. and Neville, T. (2020) Platinum(II) and Ruthenium(II) complexes in medicine: Antimycobacterial and Anti-HIV activities. *Coordination Chemistry Reviews*. **414**, 213285.

Zampar, S., Klafki, W.H., Sritharen, K., Bayer, T.A., Wiltfang, J., Rostagno, A., Ghiso, J., Miles, L.A. and Wirths, O. (2020) N-terminal heterogeneity of parenchymal and vascular amyloid-β deposits in Alzheimer's disease. *Neuropathology and Applied Neurobiology*. **46**, 673–685.

Received: February 9, 2022
Sent to Subject Editor: March 2, 2022
Accepted: July 23, 2022
Recommended by Subject Editor Sebastian Collins